Synthesis and Characterization of Polypyridine Ruthenium(II) Complexes Containing S-Bonded Thioether Ligands. X-ray Crystal Structures of *cis*- and *trans*-Bis(2,2'-bipyridine)bis(phenothiazine-*S*)ruthenium(II) Hexafluorophosphates[1]

Rudi Kroener,[2] Mary Jane Heeg,[3] and Edward Deutsch*[2]

Received April 28, 1987

A series of S-bonded thioether complexes of the general formulas *cis*- and *trans*-[(bpy)$_2$L$_2$Ru^{II}]$^{2+}$, [(terpy)L$_2$Ru^{II}Cl]$^+$, and *cis*-[(bpy)$_2$LRu^{II}Cl]$^+$ has been synthesized (bpy represents bipyridine; terpy represents terpyridine; L represents phenothiazine, 10-methylphenothiazine, diphenyl sulfide, methyl phenyl sulfide, and 1,4-dithiane). Individual complexes have been characterized by elemental analyses, reverse-phase thin-layer and high-performance liquid chromatography, visible–UV spectrophotometry, and cyclic voltammetry. One-equivalent oxidation of complexes containing S-bonded phenothiazine appears to induce rapid Ru–S bond fission and net loss of the phenothiazine ligand. The *cis*-[(bpy)$_2$(PTZ)Ru^{II}Cl]$^+$ complex undergoes solvent-dependent thermal Ru–S bond fission and very efficient photochemically induced Ru–S bond fission. Single-crystal X-ray structure analyses of the title complexes reveal (a) the lack of a structural trans effect induced by the S-bonded phenothiazine ligand and (b) the presence of stacking interactions between the bpy and phenothiazine ligands (average interplane distances 3.2 (5) and 3.0 (7) Å for the cis and trans isomers, respectively). The cis complex crystallizes as *cis*-[(bpy)$_2$(phenothiazine-S)$_2$Ru](PF$_6$)$_2$·$^1/_2$H$_2$O (formula weight 1111, RuN$_6$S$_2$C$_{44}$P$_2$F$_{12}$O$_{0.5}$H$_{35}$) in the monoclinic space group $P2_1/c$ with a = 14.705 (6) Å, b = 22.097 (7) Å, c = 27.922 (9) Å, β = 84.92 (3)°, and V = 9037 (5) Å^3, with Z = 8, for 8931 observed reflections with $I_o \geq 2\sigma(I)$. The trans complex crystallizes as *trans*-[(bpy)$_2$(phenothiazine-S)$_2$Ru](PF$_6$)$_2$·H$_2$O (formula weight 1120, RuN$_6$S$_2$C$_{44}$P$_2$F$_{12}$OH$_{36}$) in the triclinic space group $P\bar{1}$ with a = 8.019 (3) Å, b = 14.170 (2) Å, c = 19.854 (4) Å, α = 90.20 (1)°, β = 99.82 (2)°, γ = 95.89 (2)°, and V = 2211 Å^3, with Z = 2, for 5259 observed reflections with $I_o \geq 2\sigma(I)$.

Introduction

Current interest in the chemistry, reactivity, and particularly the photochemistry of polypyridine ruthenium(II) complexes arises mainly from their potential application in solar energy conversion processes.[4–10] A recent study[4] has shown that coordination of a S-bonded phenothiazine (PTZ) ligand to a polypyridine ruthenium(II) center does not eliminate the inherent luminescence of the center, even though free PTZ effectively quenches the excited state of [(bpy)$_3$Ru]$^{2+}$. It thus appears as though polypyridine ruthenium(II) complexes containing S-bonded thioether ligands may usefully extend the range of materials suitable for photochemical investigations. In this context we have extended our previous studies[11,12] by undertaking the synthesis and characterization of a variety of such complexes; emphasis has been given to complexes containing the redox-active PTZ ligand and to structural characterization of the cis and trans isomers of [(bpy)$_2$(PTZ)$_2$Ru]$^{2+}$ (where bpy represents 2,2'-bipyridine).

Acronyms and Abbreviations

The following acronyms and abbreviations are used in this article: bpy = 2,2'-bipyridine; terpy = 2,2':6',2''-terpyridine; PTZ = phenothiazine; MePTZ = 10-methylphenothiazine; DPS = diphenyl sulfide; MPS = methyl phenyl sulfide; PDT = 1,4-dithiane; TEAP = tetraethylammonium perchlorate; SSCE = saturated sodium calomel electrode; HPLC = high-performance liquid chromatography; TLC = thin-layer chromatography; CV = cyclic voltammetry/voltammogram.

Experimental Section

Materials. All common chemicals were of reagent grade and were used as received unless otherwise noted. Water was triply distilled and then filtered through charcoal. This water, HPLC-grade methanol, and HPLC-grade sodium heptanesulfonate were used to prepare TLC and

HPLC mobile phases. HPLC mobile phases were passed through a 0.45-μm filter and degassed by ultrasonication before use. Reverse-phase TLC plates with fluorescence indicator were obtained from Whatman (MKC18-F). PDT was recrystallized two times from 2-butanone. TEAP was recrystallized two times from water and then dried in vacuo at 60 °C. Silica gel for preparative chromatography (60–200 mesh) was obtained from Davison Chemical Co. Commercially available tank argon or nitrogen was purified by passage through chromous scrubbing towers.

Analyses. Elemental analyses were performed by Galbraith Laboratories, Inc., Knoxville, TN, or by MicAnal Laboratories, Tucson, AZ.

Synthesis of Complexes. *cis*-**Bis(2,2'-bipyridine)bis(thioether)ruthenium(II) Hexafluorophosphate, [(bpy)$_2$RuL$_2$](PF$_6$)$_2$, and *cis*-Bis(2,2'-bipyridine)(thioether)(X)ruthenium(II) Hexafluorophosphate, [(bpy)$_2$(X)RuL]PF$_6$(X = Cl; L = PTZ, MePTZ, MPS).** These complexes were prepared by a simple modification of the aqueous method previously described.[14] Typically, 0.26 g of *cis*-(bpy)$_2$RuCl$_2$·2H$_2$O[13] (0.50 mmol) and a 10–30-fold molar excess of a thioether ligand were added to 50 mL of 50% aqueous ethanol and the mixture was deaerated before being heated at reflux with vigorous stirring for 2.5–4 h. Prolonged reaction times yield more of the disubstituted complex. The reaction solutions gradually turned clear orange to red during the reflux period. Excess ligand was removed by filtration or diethyl ether extraction. An excess of solid ammonium hexafluorophosphate was added to precipitate the products, and the resulting yellow or orange powder was collected by filtration, washed with water and diethyl ether, and dried by suction. Purification of all complexes was effected by adsorption of a concentrated acetone or acetonitrile solution of the product mixture onto a 2 × 30 cm column containing silica gel followed by sequential elution with pure toluene and then 1/3, 1/2, 5/7, and 1/1 acetonitrile/toluene solutions. For the MPS complex only pure toluene and 1/3 acetonitrile/toluene was used. The monosubstituted complex is the first dark red band eluted under these conditions. Purified complexes were reprecipitated from acetone/diethyl ether or acetonitrile/diethyl ether and dried in vacuo at about 40 °C overnight. Relevant analytical, electrochemical, and spectrophotometric data are given in Tables I–III, respectively. Chromatographic data are given in Tables IV and V. Chloride salts can be prepared from these hexafluorophosphate salts by metathesis with tetrabutylammonium chloride in acetone.

trans-**Bis(2,2'-bipyridine)diaquoruthenium(II) Hexafluorophosphate, *trans*-[(bpy)$_2$Ru(H$_2$O)$_2$](PF$_6$)$_2$.** This complex was prepared from (bpy)$_2$RuCO$_3$·2H$_2$O[14] by following a literature preparation[15] with HPF$_6$ instead of HClO$_4$.

trans-**Bis(2,2'-bipyridine)bis(thioether)ruthenium(II) Hexafluorophosphate, *trans*-[(bpy)$_2$RuL$_2$](PF$_6$)$_2$ (L = PTZ, MePTZ, MPS, PDT).** These complexes were prepared from *trans*-[(bpy)$_2$Ru(H$_2$O)$_2$](PF$_6$)$_2$ by

(1) Abstracted in part from: Kroener, R. M.S. Thesis, University of Cincinnati, 1984.
(2) University of Cincinnati.
(3) Wayne State University.
(4) Root, M. J.; Deutsch, E. A.; Sullivan, J. C.; Meisel, D. *Chem. Phys. Lett.* **1983,** *101,* 353.
(5) Kalayanasundaran, K. *Coord. Chem. Rev.* **1982,** *46,* 159.
(6) Whitten, D. G. *Acc. Chem. Res.* **1980,** *13,* 83.
(7) Meyer, T. J. *Acc. Chem. Res.* **1978,** *11,* 94.
(8) Sutin, N. *J. Photochem.* **1979,** *10,* 19.
(9) For a recent review see: Rillema, D. P.; Taghdiri, D. G.; Jones, D. S.; Keller, C. D.; Worl, L. A.; Meyer, T. J.; Levy, H. A. *Inorg. Chem.* **1987,** *26,* 578.
(10) Chen, P.; Westmoreland, T. D.; Danielson, E.; Schanze, K. S.; Anthon, D.; Neveux, P. E., Jr.; Meyer, T. J. *Inorg. Chem.* **1987,** *26,* 1116.
(11) Root, M. J.; Deutsch, E. *Inorg. Chem.* **1985,** *24,* 1464.
(12) Root, M. J.; Sullivan, B. P.; Meyer, T. J.; Deutsch, E. *Inorg. Chem.* **1985,** *24,* 2731.

(13) Sullivan, B. P.; Salmon, D. J.; Meyer, T. J. *Inorg. Chem.* **1978,** *17,* 3334.
(14) Johnson, E. C.; Sullivan, B. P.; Salmon, D. J.; Adeyemi, S. A.; Meyer, T. J. *Inorg. Chem.* **1978,** *17,* 2211.
(15) Durham, B.; Wilson, S. R.; Hodgson, D. J.; Meyer, T. J. *J. Am. Chem. Soc.* **1980,** *102,* 600.

Table I. Elemental Analyses of Polypyridine Ruthenium(II) Complexes Containing Phenothiazine

		% C	% H	% Ru	% S	% N	% Cl	% P
cis-[(bpy)$_2$(PTZ)$_2$Ru](PF$_6$)$_2$	calcd	47.96	3.11	9.17	5.82	7.62		
	found	47.50	3.21	8.91	5.83	7.48		
cis-[(bpy)$_2$(PTZ)RuCl]PF$_6$	calcd	48.46	3.18	12.74	4.04	8.83	4.47	
	found	47.69	3.41	12.72	3.97	8.83	3.94	
trans-[(bpy)$_2$(PTZ)$_2$Ru](PF$_6$)$_2$	calcd			9.17	5.81	7.62		5.62
	found			9.34	5.61	7.44		5.38
[(bpy)(terpy)Ru(PTZ)]Cl$_2$	calcd				4.21		9.32	
	found				4.00		8.99	
[(terpy)(PTZ)$_2$RuCl]PF$_6$	calcd			11.06	7.02	7.66		3.39
	found			10.91	7.51	7.46		3.45

Table II. Electrochemical Parameters for Polypyridine Ruthenium(II) Complexes Containing Thioether Ligands

complex	$E_{1/2}^{ox}$, V vs SSCE		$E_{1/2}^{red}$, V vs SSCE	
cis-[(bpy)$_2$(PTZ)$_2$Ru](PF$_6$)$_2$	+0.58^a	+0.82^a	−1.41	−1.61
	+1.13^a	+1.43	−1.86	
trans-[(bpy)$_2$(PTZ)$_2$Ru](PF$_6$)$_2$	+0.58^a	+0.82^a	−1.38	−1.57
	+1.13^a	+1.43		
cis-[(bpy)$_2$(MePTZ)$_2$Ru](PF$_6$)$_2$	+1.11	+1.38	−1.47^c	−1.70^c
trans-[(bpy)$_2$(MePTZ)$_2$Ru](PF$_6$)$_2$	+1.12	+1.35	−1.40^c	−1.63^c
cis-[(bpy)$_2$(MPS)$_2$Ru](ClO$_4$)$_2$	+1.50		−1.38	−1.70
trans-[(bpy)$_2$(MPS)$_2$Ru](PF$_6$)$_2$	+1.46		−1.37	−1.57
cis-[(bpy)$_2$(DPS)$_2$Ru](ClO$_4$)$_2$	+1.07^a	+1.16^a	−1.42	−1.60
trans-[(bpy)$_2$(PDT)$_2$Ru](PF$_6$)$_2$	+1.07^a	+1.46	−1.35	−1.69
	+1.60^b			
[(terpy)(PTZ)$_2$RuCl]PF$_6$	+0.59^a	+0.85^a	−1.45	−1.62
	+1.10^a	+1.33^a		
[(terpy)(MePTZ)$_2$RuCl]PF$_6$	+0.73^a	+0.99^a	−1.43	−1.61
	+1.35^a			
[(terpy)(MPS)$_2$RuCl]PF$_6$	+0.92		−1.25^c	−1.47^c
			−1.81	
cis-[(bpy)$_2$(PTZ)RuCl]PF$_6$	+0.58	+0.86	−1.37^c	−1.56
	+1.11		−1.75	
cis-[(bpy)$_2$(MePTZ)RuCl]PF$_6$	+0.68	+0.88	−1.37^c	−1.53
	+1.33^a		−1.71^c	
cis-[(bpy)$_2$(MPS)RuCl]PF$_6$	+0.89		−1.36^c	−1.53
				−1.72

^{a} Irreversible anodic wave. ^{b} Irreversible anodic wave, only observed at slow scan rates. ^{c} Irreversible cathodic wave.

modification of a reported procedure.[16] To 20 mL of deaerated 50% aqueous ethanol were added 0.10 g of *trans*-[(bpy)$_2$Ru(H$_2$O)$_2$](PF$_6$)$_2$ (0.13 mmol) and a 10–30-fold molar excess of the appropriate ligand. The mixture was deaerated for 15–20 min and then heated at reflux for 1–2 h. The reaction solutions were evaporated to dryness, and the residue was extracted with about 50 mL of diethyl ether to remove excess ligand. The residue was dissolved in a minimum amount of acetonitrile, and the solution was added dropwise to about 200 mL of cold, stirred diethyl ether. Purification was effected by one or two successive reprecipitations from acetonitrile/diethyl ether. Analytical, electrochemical, and spectrophotometric data are given in Tables I–III, respectively. Chromatographic data are given in Tables IV and V.

(2,2′-Bipyridine)(2,2′:6′,2″-terpyridine)(phenothiazine)ruthenium(II) Chloride, [(bpy)(terpy)Ru(PTZ)]Cl$_2$. This complex was synthesized and purified as previously described.[5]

(2,2′:6′,2″-Terpyridine)bis(thioether)chlororuthenium(II) Hexafluorophosphate, [(terpy)(L)$_2$ClRu]PF$_6$ (L = PTZ, MePTZ, MPS). Two procedures were used to prepare the crude salts. (A) For the PTZ and MePTZ complexes, 0.22 g of (terpy)RuCl$_3$[17] (0.5 mmol) and a 30–50-fold molar excess of ligand were added to 50 mL of 80/20 (v/v) water/ethanol and the solution was deaerated for 15–20 min. The reaction mixture was heated at reflux with stirring for 17–24 h. After it was cooled, the solution was filtered to remove excess solid ligand, and the desired product was precipitated by addition of solid ammonium hexafluorophosphate. The resulting brown powder was collected by filtration, washed with water and then diethyl ether, and finally dried by suction. (B) All three complexes were prepared by substituting thioether ligands for phosphine ligands in a reported procedure.[17] A mixture of 0.22 g of (terpy)RuCl$_3$[17] (0.5 mmol), 60 mL of chloroform, 2 mL tri-

ethylamine, and a 20-fold excess of ligand were heated at reflux for 24 h. The resulting solution was evaporated to dryness and the residue dissolved in a minimum amount of warm ethanol. The desired product was precipitated by addition of a concentrated solution of ammonium hexafluorophosphate, followed by water if necessary.

Purification of the crude salts was effected with a 1/3, 1/1 acetonitrile/toluene gradient on a 2 × 30 cm column of silica gel, followed by recrystallization from acetone/diethyl ether at 0 °C. Relevant analytical, electrochemical, and spectrophotometric data are given in Tables I–III, respectively. Chromatographic data are given in Tables IV and V.

cis-**Bis(2,2′-bipyridine)bis(thioether)ruthenium(II) Perchlorate, [(bpy)$_2$RuL$_2$](ClO$_4$)$_2$ (L = MePTZ, DPS, MPS).** These complexes were prepared from *cis*-(bpy)$_2$RuCl$_2$·2H$_2$O via *cis*-[(bpy)$_2$(CH$_3$COCH$_3$)$_2$Ru]$^{2+}$ by a modification of a published procedure.[13] Typically, 0.26 g (0.5 mmol) of (bpy)$_2$RuCl$_2$·2H$_2$O[13] and 0.21 g (1.0 mmol) of AgClO$_4$ were added to 50 mL of deaerated acetone. The resultant mixture was stirred in the dark for 4.5 h and then filtered through paper. To the red-brown filtrate was added about a 10-fold molar excess of ligand, and then this solution was again deaerated and heated at reflux for about 4 h. The resulting reaction mixture was evaporated to dryness, and excess ligand was removed by extraction with diethyl ether. The residue was dissolved in a minimum amount of acetonitrile, and this was adsorbed onto a 2 × 30 cm silica column, which was subsequently eluted with pure toluene followed by 1/3, 1/2, and 1/1 acetonitrile/toluene solutions. The desired bis(thioether) complex comprises the major yellow band, which is sometimes preceded by a small red band of the mono(thioether) complex. In the case of the DPS product, orange and dark green bands of unknown composition usually follow the major yellow band. Relevant analytical, electrochemical, and spectrophotometric data are given in Tables I–III, respectively. Chromatographic data are given in Tables IV and V.

cis-**Bis(2,2′-bipyridine)bis(acetonitrile)ruthenium(II) Hexafluorophosphate, *cis*-[(bpy)$_2$(CH$_3$CN)$_2$Ru](PF$_6$)$_2$.** This complex was synthesized as previously described.[18]

cis-**(2,2′-Bipyridine)(solvent)chlororuthenium(II) Perchlorate, *cis*-[(bpy)$_2$SRuCl]ClO$_4$ (S = Acetone, Acetonitrile).** Solutions of these complexes were prepared by stirring 1 equiv of *cis*-(bpy)$_2$RuCl$_2$·2H$_2$O[13] with 1 equiv of AgClO$_4$ in the appropriate solvent in the dark for 1.5 h.[14] Filtered reaction solutions were used as spectral and TLC references during investigations of the reactivity of *cis*-[(bpy)$_2$(PTZ)RuCl]PF$_6$ in different solvents (vide infra).

Equipment. All visible and UV spectra were obtained on a Cary 210 spectrophotometer at ambient temperature.

HPLC experiments were performed on a BAS Model CS-2b system, equipped with an Alltech C$_8$ reverse-phase column (250 × 4.6 mm; 10 μm), which was serviced by a Milton-Roy minipump. The precolumn (60 × 2 mm) was packed with C$_8$-coated silica (Anspec). UV detection at 254 nm was performed with a Beckman Model 153 detector and recorded on a strip-chart recorder interfaced with a Hewlett-Packard HP 3390 integrator.

Electrochemical experiments were performed at ambient temperature in acetonitrile by using a Bioanalytical Systems CV-1A sweep generator and potentiostat and were monitored by using a Keithley Model 178 digital multimeter and a Hewlett-Packard 7015B X-Y recorder. A standard three-electrode electrochemical cell, containing a glassy-carbon working electrode, an SSCE, and a platinum wire as auxiliary electrode, was used. Reaction solutions were deaerated with a constant stream of purified nitrogen gas. Values for $E_{1/2}$ derived from CV measurements were calculated by averaging anodic and cathodic peak potentials for associated redox waves and are not corrected for junction potential.

X-ray Characterization of *cis*- and *trans*-Bis(2,2′-bipyridine)bis(phenothiazine)ruthenium(II) Hexafluorophosphate, *cis*- and *trans*-[(bpy)$_2$-

(16) Walsh, J. L.; Durham, B. *Inorg. Chem.* **1982**, *21*, 329.

(17) Sullivan, B. P.; Calvert, J. M.; Meyer, T. J. *Inorg. Chem.* **1980**, *19*, 1404.

(18) Brown, G. M.; Callahan, R. W.; Meyer, T. J. *Inorg. Chem.* **1975**, *14*, 1915.

Table III. Visible and UV Spectrophotometric Parameters in Acetonitrile for Polypyridine Ruthenium(II) Complexes Containing Thioether Ligands

complex	λ_{max}, nm (ϵ_{max}, M^{-1} cm^{-1})
cis-[(bpy)$_2$(PTZ)$_2$Ru](PF$_6$)$_2$	425 (5680), 393 (5100), 325 sh (15 100), 280 (44 000), 268 sh (33 800), 246 (43 700), 215 sh (61 600), 200 sh (78 100)
trans-[(bpy)$_2$(PTZ)$_2$Ru](PF$_6$)$_2$	456 sh (4600), 424 (7600), 363 (12 000), 289 (35 600), 270 (32 580), 250 (35 300), 221 (29 600), 200 sh (48 000)
cis-[(bpy)$_2$(MePTZ)$_2$Ru](PF$_6$)$_2$	426 (4900), 393 (4560), 325 sh (12 100), 279 (44 100), 268 (35 600), 247 (42 200), 218 sh (53 000)
trans-[(bpy)$_2$(MePTZ)$_2$Ru](PF$_6$)$_2$	456 sh (4530), 427 (6230), 362 (10 600), 351 sh (9340), 282 (31 300), 269 sh (29 300), 250 (31 300), 222 (40 000)
cis-[(bpy)$_2$(MPS)$_2$Ru](ClO$_4$)$_2$	421 (5940), 338 sh (3110), 280 (35 600), 268 sh (28 200), 250 (22 400), 237 (24 200)
trans-[(bpy)$_2$(MPS)$_2$Ru](PF$_6$)$_2$	455 sh (3820), 430 (5880), 346 (2350), 289 (40 900), 271 (35 160), 255 (38 300), 218 sh (21 500), 203 sh (68 200)
cis-[(bpy)$_2$(DPS)$_2$Ru](ClO$_4$)$_2$	416 (5200), 384 sh (4070), 345 (2650), 283 (38 700), 264 sh (17 100), 252 (18 800), 241 (21 800)
trans-[(bpy)$_2$(PDT)$_2$Ru](PF$_6$)$_2$	457 sh (5940), 431 (8280), 346 (2670), 283 (39 400), 248 sh (16 100), 238 (17 800)
[(terpy)(bpy)(PTZ)Ru]Cl$_2$	452 (8700), 427 (8900), 328 sh (18 000), 282 (45 000), 269 (34 500), 254 (26 000), 240 sh (32 500), 215 (36 200)
[(terpy)(PTZ)$_2$RuCl]PF$_6$	491 (3250), 353 (14 100), 303 (32 200), 280 (33 900), 268 (33 700), 250 (35 900), 219 sh (65 300)
[(terpy)(MePTZ)$_2$RuCl]PF$_6$	490 (4360), 354 (18 100), 303 (37 600), 272 (45 900), 268 (45 900), 252 (45 100), 219 (78 100)
[(terpy)(MPS)$_2$RuCl]PF$_6$	490 (3060), 325 sh (8410), 308 (25 700), 268 sh, 254 (32 100), 228 (26 000)
cis-[(bpy)$_2$(PTZ)RuCl]PF$_6$^{a}	486 (5240), 331 (8050), 291 (37 200), 267 sh (20 700), 255 sh (19 100)
cis-[(bpy)$_2$(MePTZ)RuCl]PF$_6$^{a}	490 (6970), 330 (12 100), 291 (26 300), 270 sh (15 300), 252 (16 600)
cis-[(bpy)$_2$(MPS)RuCl]PF$_6$^{a}	488 (5720), 339 (5890), 292 (37 300), 270 sh (11 400), 255 sh (13 500)

^{a} In CH$_2$Cl$_2$.

Table IV. Retention Factors for Reverse-Phase Ion-Pairing TLC of Selected Polypyridine Ruthenium(II) Complexes^a

complex	R_f
cis-[(bpy)$_2$(PTZ)$_2$Ru](PF$_6$)$_2$	0.25
trans-[(bpy)$_2$(PTZ)$_2$Ru](PF$_6$)$_2$	0.20
cis-[(bpy)$_2$(MePTZ)$_2$Ru](PF$_6$)$_2$	0.22
trans-[(bpy)$_2$(MePTZ)$_2$Ru](PF$_6$)$_2$	0.20
cis-[(bpy)$_2$(MPS)$_2$Ru](ClO$_4$)$_2$	0.33
trans-[(bpy)$_2$(MPS)$_2$Ru](PF$_6$)$_2$	0.30
cis-[(bpy)$_2$(DPS)$_2$Ru](ClO$_4$)$_2$	0.35
trans-[(bpy)$_2$(PDT)$_2$Ru](PF$_6$)$_2$	0.20
cis-[(bpy)$_2$(MeCN)$_2$Ru](PF$_6$)$_2$	0.36
cis-(bpy)$_2$RuCl$_2$·2H$_2$O	0.85
[(terpy)(bpy)RuCl]PF$_6$	0.46
(bpy)$_3$Ru(PF$_6$)$_2$	0.28
[(terpy)(PTZ)$_2$RuCl]PF$_6$	0.18
[(terpy)(MePTZ)$_2$RuCl]PF$_6$	0.18
[(terpy)(MPS)$_2$RuCl]PF$_6$	0.32
[(terpy)(bpy)(PTZ)Ru]Cl$_2$	0.28
cis-[(bpy)$_2$(PTZ)RuCl]PF$_6$	0.40
cis-[(bpy)$_2$(MePTZ)RuCl]PF$_6$	0.40
cis-[(bpy)$_2$(MPS)RuCl]PF$_6$	0.55
cis-[(bpy)$_2$((CH$_3$)$_2$CO)RuCl]PF$_6$	0.66
cis-[(bpy)$_2$(MeCN)RuCl]PF$_6$	0.64
cis-[(bpy)$_2$(MeOH)RuCl]PF$_6$	0.70
cis-[(bpy)$_2$(EtOH)RuCl]PF$_6$	0.70
phenothiazine	0.30

^{a} Conditions: Whatman MKC$_{18}$-F TLC plates with fluorescent indicator; 75/25 methanol/water, 0.02 M sodium heptanesulfonate mobile phase.

Table V. Retention Times and Retention Volumes for Reverse-Phase Ion-Pairing HPLC of Selected Polypyridine Ruthenium(II) Complexes^a

complex	T_R, min	V_R, mL
cis-[(bpy)$_2$(PTZ)RuCl]PF$_6$	4.7	7.0
cis-[(bpy)$_2$(MePTZ)RuCl]PF$_6$	4.8	7.1
cis-[(bpy)$_2$(MPS)RuCl]PF$_6$	4.5	6.7
cis-[(bpy)$_2$(MTZ)$_2$Ru](PF$_6$)$_2$	11.2	16.8
trans-[(bpy)$_2$(PTZ)$_2$Ru](PF$_6$)$_2$	12.7	19.1
cis-[(bpy)$_2$(MePTZ)$_2$Ru](PF$_6$)$_2$	11.3	17.0
trans-[(bpy)$_2$(MePTZ)$_2$Ru](PF$_6$)$_2$	12.8	19.2
cis-[(bpy)$_2$(MPS)$_2$Ru](ClO$_4$)$_2$	9.8	14.7
trans-[(bpy)$_2$(MPS)$_2$Ru](PF$_6$)$_2$	10.9	16.3
cis-[(bpy)$_2$(DPS)$_2$Ru](ClO$_4$)$_2$	10.6	15.9
trans-[(bpy)$_2$(PDT)$_2$Ru](PF$_6$)$_2$	12.6	18.9
cis-[(bpy)$_2$(MeCN)$_2$Ru](PF$_6$)$_2$	7.8	11.7
[(terpy)(bpy)(PTZ)Ru]Cl$_2$	8.9	13.3
[(terpy)(PTZ)$_2$RuCl]PF$_6$	6.4	9.7
[(terpy)(MePTZ)$_2$RuCl]PF$_6$	6.6	9.9
[(terpy)(MPS)$_2$RuCl]PF$_6$	5.8	8.6

^{a} Conditions: 75/25 methanol/water, 0.02 M sodium heptanesulfonate mobile phase; 1700–1800 psi; 1.5 mL/min flow rate.

(PTZ)$_2$Ru](PF$_6$)$_2$. Single crystals of the cis isomer were grown by slow evaporation of an acetone/xylene (Fisher X-4) solution at about 5 °C. Single crystals of the trans isomer were grown by slow evaporation of an acetonitrile/xylene solution at room temperature. In both cases the interior of the containing vessel was coated with a trace of silicon grease to prevent the bright orange-red crystals from sticking to the glass surface.

Data collection was performed on a Nonius CAD-4 automated diffractometer equipped with Mo Kα radiation (λ = 0.710 69 Å) and a graphite monochromator. Three monitor reflections were checked every 200 observations for intensity and every 2 h for orientation. Variation in intensity over the entire data collection was <3% in each case. The structures were solved by heavy-atom methods and refined with the use of SHELX[19] programs. The function minimized was $\sum w(F_o - |F_c|)^2$. Blocked matrices were used in the final cycles. Hydrogen atoms were placed in a combination of observed and calculated positions and held

invariant; all non-hydrogen atoms were refined anisotropically. Some disorder was evident in the hexafluorophosphate anions of both structures, with residual electron density representing up to 1.3 e Å^{-3}. No absorption corrections or corrections for secondary extinction were made. Neutral-atom scattering factors and corrections for anomalous dispersion were from ref 20. Other details are given in Table VI.

Results

Characterization. The ruthenium(II) complexes prepared in this study are characterized by (a) satisfactory elemental analyses for at least one member of each class of compounds (Table I), (b) the methods of preparation, (c) cyclic voltammetry parameters (Table II), (d) visible and ultraviolet spectrophotometric parameters (Table III), (e) reverse-phase ion-pairing TLC (Table IV) and HPLC (Table V) parameters, and (f) single-crystal X-ray structural analyses of the cis and trans isomers of [(bpy)$_2$-(PTZ)$_2$Ru](PF$_6$)$_2$ (vide infra).

The CV studies reveal both the Ru(II)/Ru(III) couple and the ligand-based redox processes that are characteristic for polypyridine ruthenium(II) complexes.[11-13,21] Peak potential separations for the Ru(II)/Ru(III) couple vary from 60 to 105 mV

(19) All computations were performed with local modifications of the programs of SHELX-76; Sheldrick, G. M. "SHELX-76"; University Chemical Laboratory: Cambridge, England, 1976.

(20) *International Tables for Crystallography*; Kynoch: Birmingham, England, 1974; Vol. 4 (present distributor D. Reidel, Dordrecht, The Netherlands).

(21) Callahan, R. W.; Keene, F. R.; Meyer, T. J.; Salmon, D. J. *J. Am. Chem. Soc.* **1977**, *99*, 1064.

Table VI. Experimental Crystallographic Data

	cis-[(bpy)$_2$(PTZ)$_2$Ru](PF$_6$)$_2$·$^1/_2$H$_2$O	trans-[(bpy)$_2$(PTZ)$_2$Ru](PF$_6$)$_2$·H$_2$O
formula	RuN$_6$S$_2$C$_{44}$P$_2$F$_{12}$H$_{35}$O$_{0.5}$	RuN$_6$S$_2$C$_{44}$P$_2$F$_{12}$H$_{36}$O
mol wt	1110.93	1119.94
cryst dimens	0.40 × 0.40 × 0.50 mm	0.15 × 0.18 × 0.20 mm
cryst syst	monoclinic	triclinic
space group	$P2_1/c$	$P\bar{1}$
a, Å	14.705 (6)	8.019 (3)
b, Å	22.097 (7)	14.170 (2)
c, Å	27.922 (9)	19.854 (4)
α, deg		90.20 (1)
β, deg	84.92 (3)	99.82 (2)
γ, deg		95.89 (2)
V, Å^3	9037 (5)	2211 (1)
Z	8	2
ρ(calcd), g cm^{-3}	1.633	1.682
2θ range, deg	3–50	3–52
max scan time, s	45	45
scan angle, deg	1.0 ± 0.2 tan θ	0.9 + 0.2 tan θ
temp	ambient	138 (2) K
octants collected	$0 \leq h \leq 17, 0 \leq k \leq 26,$ $-33 \leq l \leq 33$	$0 \leq h \leq 9, -17 \leq k \leq 17,$ $-24 \leq l \leq 24$
total no. of data	16 502	8867
no. of obsd data, $I_o > 2\sigma(I)$	8931	5259
μ(Mo kα), cm^{-1}	5.4	5.5
F_{000}	4472	1128
R	0.068	0.064
$R_w{}^a$	0.069	0.062

$^a R_w = [\sum w(|F_o| - |F_c|)^2 / \sum w F_o^2]^{1/2}$; $w = (\sigma_F)^{-2}$.

and are virtually independent of scan rate. While these separations are larger than the ideal Nernstian value of 59 mV, such values are commonly observed for complexes of this type,[11-13,21] presumably due to solution resistance. Plots of peak current versus the square root of the scan rate are linear, indicating that the electrode processes involved in the Ru(II)/Ru(III) couple are diffusion-controlled.

The visible–UV spectra of these complexes exhibit the intense bands that are characteristic of polypyridine ruthenium(II) complexes.[11-13,22-27] Figure 1 compares the visible–UV spectra of three bis(phenothiazine) complexes: cis- and trans-[(bpy)$_2$(PTZ)$_2$Ru]$^{2+}$ and [(terpy)(PTZ)$_2$RuCl]$^+$.

Crystal Structure of cis-[(bpy)$_2$(PTZ)$_2$Ru](PF$_6$)$_2$·$^1/_2$H$_2$O. Fractional atomic coordinates are given in Table VII. The asymmetric unit contains two complete independent cations, four anions, and one molecule of water. All atoms occupy general positions. The two independent cations are chemically equivalent; therefore, only averaged select bond lengths and angles are presented in Table VIII. Full listings of bond lengths and angles have been deposited as supplementary material. The cis-octahedral coordination about Ru is comprised of two sets of "stacked" ligands, each set containing a bidentate bpy group and a monodentate PTZ ligand with their ring structures roughly coincident and parallel. The two sets of ligands are roughly perpendicular. Figure 2 illustrates the geometry about Ru. Distortions from ideal octahedral geometry are due primarily to the customary N–Ru–N bite angle of the bipyridine ligand (bite angle averages 78.7 (3)°). In addition, the S–Ru–S angles are significantly less than 90° (S1–Ru–S2 = 86.02 (7)°, S3–Ru–S4 = 85.81 (7)°) while all S–Ru–N angles are greater than 90°. Intramolecular close contacts do occur (see Figure 2) between the aromatic C–H group β to the sulfur atom of PTZ and the C–H group α to the N atom of the perpendicularly inclined bipyridine. Contact distances are
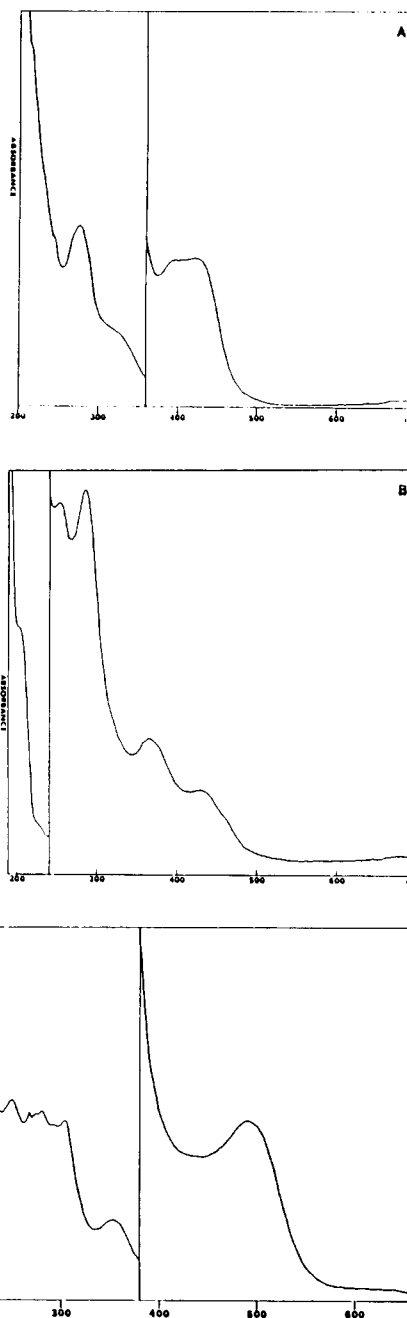
(22) Kober, E. M.; Sullivan, B. P.; Dressick, W. J.; Caspar, J. V.; Meyer, T. J. *J. Am. Chem. Soc.* **1980**, *102*, 7383.
(23) Fergusson, J. E.; Harris, G. M. *J. Chem. Soc. A* **1966**, 1293.
(24) Pankuch, B. J.; Lacky, D. E.; Crosby, G. A. *J. Phys. Chem.* **1981**, *103*, 2238.
(25) Ceulemanns, A.; Vanquickenborne, L. G. *J. Am. Chem. Soc.* **1981**, *103*, 2238.
(26) Felix, F.; Ferguson, J.; Guedel, H. K.; Ludi, A. *J. Am. Chem. Soc.* **1980**, *102*, 4096.
(27) Mayoh, B.; Day, P. *Theor. Chim. Acta* **1978**, *47*, 259.

Figure 1. Visible–UV spectra in acetonitrile at ambient temperature (path length 1.0 cm): (a) 6 × 10^{-5} M cis-[(bpy)$_2$(PTZ)$_2$Ru](PF$_6$)$_2$; (B) 3 × 10^{-5} M trans-[(bpy)$_2$(PTZ)$_2$Ru](PF$_6$)$_2$; (C) 1 × 10^{-4} M [(terpy)(PTZ)$_2$RuCl]PF$_6$.
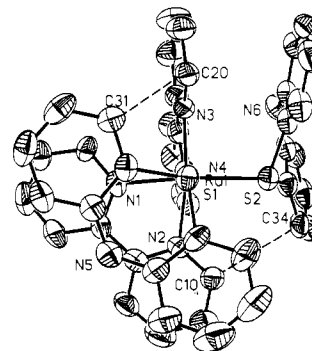

Figure 2. ORTEP drawing of one of the two independent cis-[(bpy)$_2$(PTZ)$_2$Ru]$^{2+}$ cations viewed down the S(1)–Ru(1) bond. Close contacts between the aromatic C–H linkages are indicated by the dashed lines. The orientation of the ligand ring overlap is evident, as is the fold in the PTZ ligand containing S(2). Ellipsoids are drawn at 50% probability.

Table VII. Atomic Positional Parameters of *cis*-[(bpy)₂(PTZ)₂Ru](PF₆)₂·¹/₂H₂O^{a,b}

atom	x	y	z	atom	x	y	z
Ru1	-0.00781 (4)	0.25231 (3)	0.17170 (2)	C51	0.4954 (6)	0.5159 (4)	0.3947 (3)
S1	0.1191 (1)	0.26404 (9)	0.21743 (7)	C52	0.4522 (6)	0.5429 (4)	0.4355 (4)
S2	0.1016 (1)	0.22758 (9)	0.10590 (7)	C53	0.3940 (6)	0.5090 (4)	0.4654 (3)
N1	-0.1022 (4)	0.2657 (3)	0.2307 (2)	C54	0.3815 (5)	0.4493 (4)	0.4550 (3)
N2	-0.0303 (4)	0.1647 (3)	0.1960 (2)	C55	0.3683 (7)	0.2112 (4)	0.3483 (3)
N3	-0.0133 (4)	0.3422 (3)	0.1510 (2)	C56	0.3853 (9)	0.1539 (5)	0.3332 (4)
N4	-0.1183 (4)	0.2511 (3)	0.1308 (2)	C57	0.464 (1)	0.1257 (6)	0.3447 (4)
N5	0.0405 (4)	0.1970 (3)	0.3053 (2)	C58	0.5233 (8)	0.1548 (5)	0.3719 (4)
N6	0.0196 (5)	0.3090 (3)	0.0346 (2)	C59	0.5049 (7)	0.2140 (4)	0.3868 (3)
C1	-0.1284 (5)	0.3203 (4)	0.2484 (3)	C60	0.5608 (6)	0.2495 (4)	0.4167 (3)
C2	-0.1920 (6)	0.3260 (5)	0.2885 (3)	C61	0.6405 (7)	0.2279 (5)	0.4329 (4)
C3	-0.2278 (6)	0.2740 (5)	0.3090 (3)	C62	0.6881 (7)	0.2662 (6)	0.4608 (4)
C4	-0.2041 (6)	0.2180 (5)	0.2906 (3)	C63	0.6555 (7)	0.3225 (5)	0.4729 (4)
C5	-0.1381 (5)	0.2144 (4)	0.2514 (3)	C64	0.5756 (6)	0.3415 (4)	0.4558 (3)
C6	-0.0994 (5)	0.1578 (4)	0.2312 (3)	C65	0.2337 (5)	0.4228 (4)	0.3752 (3)
C7	-0.1265 (6)	0.1013 (4)	0.2489 (3)	C66	0.1717 (5)	0.4242 (4)	0.4147 (3)
C8	-0.0827 (8)	0.0516 (5)	0.2298 (4)	C67	0.1410 (6)	0.4788 (5)	0.4342 (4)
C9	-0.0101 (7)	0.0575 (4)	0.1950 (4)	C68	0.1711 (7)	0.5319 (5)	0.4132 (4)
C10	0.0135 (6)	0.1139 (4)	0.1784 (3)	C69	0.2330 (6)	0.5311 (5)	0.3730 (4)
C11	-0.1644 (5)	0.2021 (4)	0.1200 (3)	C70	0.2645 (6)	0.4765 (5)	0.3524 (3)
C12	-0.2440 (6)	0.2064 (5)	0.0960 (3)	C71	0.3364 (6)	0.4285 (5)	0.2805 (3)
C13	-0.2749 (6)	0.2617 (5)	0.0828 (3)	C72	0.3694 (7)	0.4389 (6)	0.2328 (4)
C14	-0.2247 (6)	0.3125 (5)	0.0921 (3)	C73	0.3781 (8)	0.3918 (8)	0.2011 (4)
C15	-0.1463 (5)	0.3057 (4)	0.1170 (3)	C74	0.3562 (8)	0.3325 (7)	0.2146 (4)
C16	-0.0886 (6)	0.3574 (4)	0.1289 (3)	C75	0.3218 (6)	0.3222 (6)	0.2614 (3)
C17	-0.1058 (7)	0.4165 (5)	0.1159 (3)	C76	0.3144 (6)	0.3695 (5)	0.2939 (3)
C18	-0.0427 (8)	0.4613 (4)	0.1253 (4)	C77	0.3627 (5)	0.2891 (4)	0.5167 (3)
C19	0.0329 (7)	0.4459 (4)	0.1479 (3)	C78	0.3620 (6)	0.3311 (4)	0.5526 (3)
C20	0.0465 (6)	0.3866 (4)	0.1595 (3)	C79	0.4129 (7)	0.3182 (5)	0.5914 (3)
C21	-0.1560 (5)	0.1934 (4)	0.2375 (3)	C80	0.4617 (7)	0.2664 (5)	0.5931 (4)
C22	0.2260 (6)	0.1629 (5)	0.2106 (3)	C81	0.4590 (6)	0.2232 (5)	0.5577 (3)
C23	0.2484 (8)	0.1055 (5)	0.2233 (4)	C82	0.4070 (5)	0.2338 (4)	0.5197 (3)
C24	0.1998 (9)	0.0773 (5)	0.2621 (4)	C83	0.3200 (6)	0.1818 (4)	0.4621 (3)
C25	0.1308 (7)	0.1082 (4)	0.2900 (4)	C84	0.2953 (7)	0.1247 (4)	0.4467 (3)
C26	0.1085 (6)	0.1667 (4)	0.2785 (3)	C85	0.2125 (9)	0.1201 (6)	0.4238 (3)
C27	0.0408 (5)	0.2591 (4)	0.3104 (3)	C86	0.1592 (8)	0.1687 (6)	0.4178 (4)
C28	0.0009 (6)	0.2878 (4)	0.3520 (3)	C87	0.1844 (6)	0.2249 (5)	0.4317 (3)
C29	0.0027 (6)	0.3492 (5)	0.3573 (3)	C88	0.2660 (6)	0.2318 (4)	0.4530 (3)
C30	0.0457 (6)	0.3850 (4)	0.3211 (4)	P1	0.5833 (2)	0.1554 (1)	0.2130 (1)
C31	0.0871 (5)	0.3580 (4)	0.2795 (3)	F1	0.5803 (5)	0.1301 (3)	0.1606 (2)
C32	0.0821 (5)	0.2964 (4)	0.2742 (3)	F2	0.5876 (5)	0.1812 (3)	0.2644 (2)
C33	0.0441 (5)	0.2040 (4)	0.0553 (3)	F3	0.4821 (5)	0.1707 (5)	0.2150 (3)
C34	0.0341 (6)	0.1433 (4)	0.0468 (3)	F4	0.6868 (5)	0.1406 (5)	0.2079 (3)
C35	-0.0201 (7)	0.1255 (5)	0.0110 (4)	F5	0.6053 (8)	0.2175 (4)	0.1915 (3)
C36	-0.0648 (6)	0.1689 (5)	-0.0148 (3)	F6	0.5590 (9)	0.0930 (4)	0.2332 (3)
C37	-0.0507 (6)	0.2302 (4)	-0.0074 (3)	P2	0.8679 (2)	0.1095 (1)	0.4167 (1)
C38	0.0047 (5)	0.2485 (4)	0.0275 (3)	F7	0.8644 (7)	0.1760 (3)	0.4002 (3)
C39	0.1003 (5)	0.3304 (4)	0.0516 (3)	F8	0.8680 (7)	0.0439 (3)	0.4302 (3)
C40	0.1313 (6)	0.3890 (4)	0.0392 (3)	F9	0.9377 (6)	0.0984 (4)	0.3726 (3)
C41	0.2112 (7)	0.4103 (4)	0.0556 (3)	F10	0.7999 (7)	0.1243 (4)	0.4589 (3)
C42	0.2617 (7)	0.3744 (5)	0.0839 (3)	F11	0.7903 (7)	0.1023 (6)	0.3855 (4)
C43	0.2306 (6)	0.3169 (4)	0.0977 (3)	F12	0.9422 (7)	0.1199 (5)	0.4482 (4)
C44	0.1490 (5)	0.2960 (4)	0.0820 (3)	P3	0.3985 (4)	-0.0474 (2)	0.3873 (2)
Ru2	0.41236 (4)	0.33173 (3)	0.39652 (2)	F13	0.4354 (6)	0.0043 (4)	0.4178 (4)
S3	0.2812 (1)	0.3518 (1)	0.35573 (7)	F14	0.4570 (6)	-0.0245 (4)	0.3421 (4)
S4	0.3075 (1)	0.3047 (1)	0.46354 (7)	F15	0.3194 (9)	-0.0069 (9)	0.3749 (6)
N7	0.4984 (4)	0.3648 (3)	0.3399 (2)	F16	0.365 (1)	-0.0972 (6)	0.3573 (4)
N8	0.4226 (4)	0.4219 (3)	0.4161 (2)	F17	0.477 (1)	-0.0835 (7)	0.4054 (5)
N9	0.4268 (5)	0.2420 (3)	0.3743 (2)	F18	0.345 (1)	-0.0703 (6)	0.4344 (4)
N10	0.5281 (4)	0.3063 (3)	0.4288 (2)	P4	0.2070 (2)	-0.0134 (1)	0.0938 (1)
N11	0.3262 (5)	0.4762 (4)	0.3114 (3)	F19	0.1041 (6)	-0.0095 (6)	0.0933 (4)
N12	0.3990 (5)	0.1888 (3)	0.4849 (2)	F20	0.1995 (8)	-0.0712 (6)	0.0733 (7)
C45	0.5308 (5)	0.3330 (4)	0.3003 (3)	F21	0.2229 (8)	0.0221 (6)	0.0485 (3)
C46	0.5822 (6)	0.3588 (5)	0.2631 (4)	F22	0.200 (1)	0.0470 (4)	0.1170 (4)
C47	0.6049 (6)	0.4186 (5)	0.2658 (4)	F23	0.3054 (5)	-0.0225 (7)	0.0916 (4)
C48	0.5746 (6)	0.4519 (4)	0.3060 (3)	F24	0.1914 (9)	-0.0356 (5)	0.1439 (4)
C49	0.5211 (5)	0.4234 (4)	0.3422 (3)	O(W)	0.5267 (9)	0.0835 (5)	0.4855 (5)
C50	0.4809 (5)	0.4553 (4)	0.3855 (3)				

^{a} The estimated error in the last digit is given in parentheses. This form is used throughout. ^{b} The numbering scheme is shown in Figure 2.

H10···H34 = 2.33 (1) Å, H2O···H31 = 2.15 (1) Å, H54···H78 = 2.29 (1) Å, and H55···H75 = 2.11 (1) Å.

Crystal Structure of *trans*-[(bpy)₂(PTZ)₂Ru](PF₆)₂·H₂O. Fractional atomic coordinates are given in Table IX. The asymmetric unit contains two independent half-cations, two anions, and one molecule of water. Both independent Ru atoms occupy crystallographic centers of symmetry. Selected averaged bond lengths and angles are presented in Table VIII. Full listings of bond lengths and angles have been deposited as supplementary material. Like the cis isomer, the ligands orient to form sets of (bpy + PTZ) stacks. Due to the crystallographic inversion center, these sets are required to be mutually parallel, forming the tiered

Table VIII. Selected Averaged Bond Lengths (Å) and Angles (deg)[a]

cis-[(bpy)₂(PTZ)₂Ru]²⁺			
Ru–S	2.381 (16)	S–Ru–S	85.9 (1)
Ru–N(trans to N)	2.075 (6)	S–Ru–N(cis)	93.9 (1.8)
Ru–N(trans to S)	2.072 (6)	S–Ru–N(trans)	174.4 (5)
Ru–N(all)	2.073 (6)	N–Ru–N(bite)	78.7 (3)
S–C	1.78 (1)	Ru–S–C	109.8 (1.6)
C–N(PTZ)	1.38 (2)	Ru–N–C(bpy,inner)	115.1 (7)
C–C(PTZ)	1.39 (2)	Ru–N–C(bpy,outer)	126.1 (1.0)
C–N(bpy)	1.35 (2)	C–S–C(PTZ)	99.0 (5)
C–C(bpy,aromatic)	1.38 (1)	C–N–C(PTZ)	122.3 (8)
C–C(bpy,bridging)	1.47 (1)	C–N–C(bpy)	118.8 (9)
P–F	1.52 (4)		

trans-[(bpy)₂(PTZ)₂Ru]²⁺			
Ru–S	2.347 (2)	S–Ru–N[b]	94.3 (8)
Ru–N	2.091 (9)	N–Ru–N(bite)	77.0 (2)
S–C	1.772 (9)	Ru–S–C	109.5 (0)
C–N(PTZ)	1.39 (1)	Ru–N–C(bpy,inner)	115.1 (6)
C–C(PTZ)	1.39 (2)	Ru–N–C(bpy,outer)	127.9 (8)
C–N(bpy)	1.36 (2)	C–S–C(PTZ)	100.0 (4)
C–C(bpy,aromatic)	1.38 (2)	C–N–C(PTZ)	122.2 (7)
C–C(bpy,bridging)	1.47 (1)	C–N–C(bpy)	116.9 (4)
P–F	1.58 (1)		

[a] The esd's in parentheses represent the error calculated by averaging multiple entries and not the crystallographic error in a single measurement. [b] Does not include the symmetry-related S–Ru–N'.
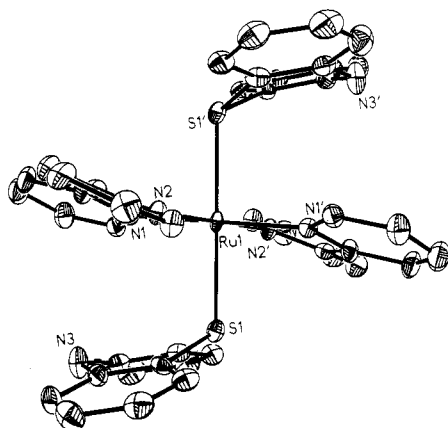

Figure 3. ORTEP drawing of the *trans*-[(bpy)₂(PTZ)₂Ru]²⁺ cation showing the tiered arrangement of the aromatic ligands. The bowing of the bpy groups and the folding of the PTZ ligand is evident. Ellipsoids are drawn at 50% probability.

structure illustrated in Figure 3. The S–Ru–N angle formed between layered ligands is slightly obtuse (94.3 (8)° average); obviously the supplementary angle describes the symmetry-related S–Ru–N' angle. The small N–Ru–N bpy bite angle is usual (77.0 (2)° average). Intramolecular close contacts occur between α-hydrogen atoms of the bpy groups, i.e. HC1···HC10' = 1.88 (1) Å and HC23···HC32' = 1.79 (1) Å.

Discussion

Synthesis and Reactivity. The synthetic procedures used in this work have been previously applied to the preparation of polypyridine ruthenium(II) complexes containing ligands with nitrogen-,[28,29] phosphorus-,[13] and sulfur-donating[11,12] atoms. It was found that the application of these general procedures was greatly facilitated by the use of reverse-phase TLC and HPLC to monitor reaction mixtures and establish product purity (Tables IV and V). For instance, it could easily be determined that the preparation of *trans*-[(bpy)₂(PTZ)₂Ru]²⁺ from *trans*-[(bpy)₂(H₂O)₂Ru]²⁺ proceeds without isomerization to the more stable cis isomer on the basis of HPLC which readily resolves and detects the cis and

(28) Dwyer, F. P.; Goodwin, H. A.; Gyarfas, E. C. *Aust. J. Chem.* **1963,** *16,* 544.
(29) Bryant, G. M.; Fergusson, J. E.; Powell, H. K. J. *Aust. J. Chem.* **1971,** *24,* 257.

Table IX. Atomic Positional Parameters of *trans*-[(bpy)₂(PTZ)₂Ru](PF₆)₂·H₂O[a]

atom	x	y	z
Ru1	0.0	0.0	0.0
S1	0.2969 (2)	0.0249 (1)	0.03367 (9)
N1	−0.0440 (7)	−0.0349 (4)	0.0975 (3)
N2	−0.0398 (7)	0.1310 (4)	0.0407 (3)
N3	0.3438 (9)	0.0441 (4)	0.1900 (3)
C1	−0.0188 (9)	−0.1160 (5)	0.1315 (4)
C2	−0.070 (1)	−0.1367 (5)	0.1922 (4)
C3	−0.153 (1)	−0.0703 (6)	0.2224 (4)
C4	−0.175 (1)	0.0148 (5)	0.1904 (4)
C5	−0.1207 (9)	0.0320 (5)	0.1292 (3)
C6	−0.1198 (9)	0.1245 (5)	0.0964 (4)
C7	−0.179 (1)	0.2031 (5)	0.1225 (4)
C8	−0.149 (1)	0.2903 (5)	0.0945 (4)
C9	−0.059 (1)	0.2986 (5)	0.0418 (4)
C10	−0.008 (1)	0.2175 (5)	0.0166 (4)
C11	0.3613 (9)	−0.0602 (4)	0.0950 (4)
C12	0.3931 (9)	−0.1477 (5)	0.0707 (4)
C13	0.431 (1)	−0.2193 (5)	0.1152 (4)
C14	0.436 (1)	−0.2056 (6)	0.1840 (4)
C15	0.408 (1)	−0.1176 (6)	0.2093 (4)
C16	0.3716 (9)	−0.0438 (5)	0.1639 (4)
C17	0.3672 (9)	0.1279 (5)	0.1550 (4)
C18	0.402 (1)	0.2141 (5)	0.1915 (4)
C19	0.425 (1)	0.2977 (5)	0.1574 (4)
C20	0.414 (1)	0.3000 (5)	0.0877 (4)
C21	0.3819 (9)	0.2153 (5)	0.0507 (4)
C22	0.3569 (9)	0.1305 (5)	0.0847 (4)
Ru2	0.50000	0.50000	0.50000
S2	0.2085 (2)	0.4906 (1)	0.45570 (9)
N4	0.5572 (8)	0.6329 (4)	0.4583 (3)
N5	0.5730 (8)	0.4657 (4)	0.4076 (3)
N6	0.2273 (9)	0.5311 (4)	0.3068 (3)
C23	0.5614 (9)	0.3784 (5)	0.3783 (4)
C24	0.647 (1)	0.3612 (5)	0.3262 (4)
C25	0.740 (1)	0.4329 (6)	0.2994 (4)
C26	0.742 (1)	0.5240 (5)	0.3245 (4)
C27	0.6581 (9)	0.5378 (5)	0.3788 (4)
C28	0.640 (1)	0.6328 (5)	0.4054 (4)
C29	0.699 (1)	0.7158 (6)	0.3758 (4)
C30	0.669 (1)	0.8020 (6)	0.4004 (5)
C31	0.577 (1)	0.8027 (5)	0.4525 (4)
C32	0.520 (1)	0.7197 (5)	0.4799 (4)
C33	0.163 (1)	0.5970 (5)	0.4125 (4)
C34	0.127 (1)	0.6716 (6)	0.4502 (4)
C35	0.118 (1)	0.7616 (6)	0.4199 (4)
C36	0.147 (1)	0.7727 (6)	0.3539 (5)
C37	0.178 (1)	0.6962 (6)	0.3156 (4)
C38	0.191 (1)	0.6070 (6)	0.3450 (4)
C39	0.180 (1)	0.4379 (5)	0.3210 (4)
C40	0.150 (1)	0.3677 (6)	0.2687 (4)
C41	0.106 (1)	0.2757 (6)	0.2817 (5)
C42	0.085 (1)	0.2472 (6)	0.3464 (5)
C43	0.114 (1)	0.3134 (6)	0.3990 (4)
C44	0.162 (1)	0.4086 (5)	0.3866 (4)
P1	0.6446 (4)	0.0895 (2)	0.3806 (1)
F11	0.7641 (8)	0.1769 (4)	0.4171 (3)
F12	0.523 (1)	0.0039 (4)	0.3425 (4)
F13	0.6770 (8)	0.1304 (4)	0.3083 (2)
F14	0.6162 (9)	0.0482 (4)	0.4509 (3)
F15	0.8024 (9)	0.0320 (4)	0.3817 (3)
F16	0.4863 (8)	0.1493 (4)	0.3759 (4)
P2	−0.1680 (3)	0.5845 (1)	0.1245 (1)
F21	0.0058 (8)	0.6521 (4)	0.1285 (3)
F22	−0.2584 (8)	0.6570 (4)	0.0751 (3)
F23	−0.2144 (9)	0.6403 (4)	0.1870 (3)
F24	−0.3395 (8)	0.5171 (4)	0.1222 (3)
F25	−0.0757 (8)	0.5149 (4)	0.1763 (3)
F26	−0.127 (1)	0.5298 (4)	0.0619 (3)
O1	0.326 (1)	0.5460 (5)	0.1724 (3)

[a] The numbering scheme is shown in Figure 3.

trans forms of [(bpy)₂(PTZ)₂Ru]²⁺ (Table V). TLC is especially useful in detecting impurities that do not elute from the HPLC column. The [(bpy)₃Ru]²⁺ complex is easily identified on TLC plates due to its red luminescence under UV illumination; under
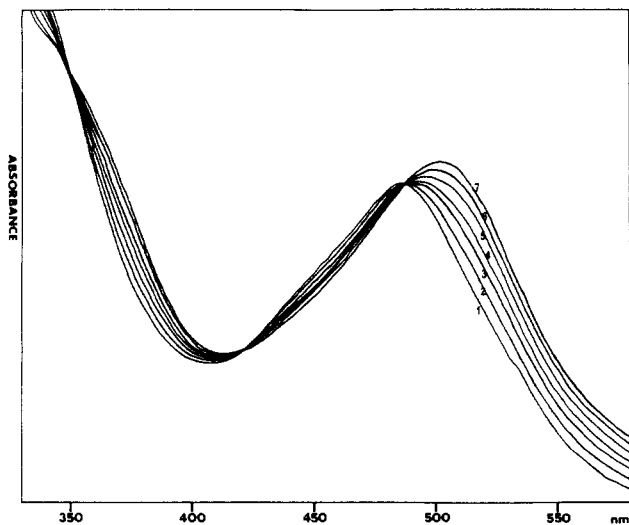
Figure 4. Sequential scans of the visible–UV spectrum of 1×10^{-4} M *cis*-[(bpy)$_2$(PTZ)RuCl]PF$_6$ in acetone at ambient temperature (path length 1.0 cm). The cell was exposed to room light for approximately 7 min between each scan.

the HPLC conditions specified in Table V, the retention time of [(bpy)$_3$Ru]$^{2+}$ is significantly longer (ca. 36 min) than that of any of the thioether derivatives.

Syntheses of the diphenyl sulfide (DPS) complexes proved to be more difficult than those of the other thioether complexes, presumably because of the steric requirements of this particular ligand. Direct substitution of DPS onto *cis*-(bpy)$_2$RuCl$_2$ in ethanol/water affords only small yields of the monosubstituted derivative and no detectable yields of the disubstituted derivative. An attempt was made to prepare the monosubstituted derivative by stirring *cis*-[(bpy)$_2$((CH$_3$)$_2$CO)RuCl]$^+$ and a 2.5-fold molar excess of DPS in acetone overnight in the dark since this procedure succeeds with analogous phosphine complexes.[13] However, with DPS the major product is the chloro-bridged dimer [(bpy)$_2$RuCl$_2$R(bpy)$_2$]$^{2+}$, and only trace amounts of the desired product can be detected by TLC. From this result it appears as though DPS does not effectively compete with a coordinated chloride ligand for the labile coordination site in *cis*-[(bpy)$_2$-((CH$_3$)$_2$CO)RuCl]$^+$. With use of a 40-fold excess of DPS and more stringent reaction conditions, this synthetic route leads to a mixture of the mono- and disubstituted DPS products, which may then be separated by column chromatography. The disubstituted DPS derivative can also be cleanly prepared from *cis*-[(bpy)$_2$((CH$_3$)$_2$CO)$_2$Ru]$^{2+}$.

The complex *cis*-[(bpy)$_2$(PTZ)RuCl]$^+$ is both thermally and photochemically reactive. The thermal reactivity of this material is greatest in acetonitrile and acetone, less in methanol and ethanol, and least in dimethyl sulfoxide and *N,N*-dimethylformamide. HPLC, TLC, and spectrophotometric analyses show that in all of the first four solvents the thermal reaction proceeds by initial loss of PTZ to yield *cis*-[(bpy)$_2$(solvent)RuCl]$^+$. In methanol and ethanol the reaction stops at this stage, in acetone this mono(solvent) intermediate dimerizes to form *cis*-[(bpy)$_2$RuCl$_2$Ru-(bpy)$_2$]$^{2+}$, and in acetonitrile this mono(solvent) intermediate loses chloride to form *cis*-[(bpy)$_2$(CH$_3$CN)$_2$Ru]$^{2+}$. This final product from thermal solvation in acetonitrile has been isolated and characterized by single-crystal X-ray structural analysis.[30] Solutions of the *cis*-[(bpy)$_2$(PTZ)RuCl]$^+$ complex in acetone or dichloromethane are very photosensitive. When kept in the dark, an acetone solution of this complex exhibits no changes in spectrophotometric properties. However, even 1-min exposures to room light engender detectable absorption changes in the visible–UV region. Figure 4 illustrates the spectrophotometric changes engendered in an acetone solution of *cis*-[(bpy)$_2$(PTZ)RuCl]$^+$ upon

seven successive 7-min exposures to room light. The wavelength of maximum absorption shifts from 487 to 505 nm, while isosbestic points are maintained at 488, 421, and 348 nm. These observations suggest that the photochemically induced reaction has the same stoichiometry as does the thermal reaction, i.e. loss of PTZ from the starting material (λ_{max} = 487 nm) to form *cis*-[(bpy)$_2$-((CH$_3$)$_2$CO)RuCl]$^+$ (λ_{max} = 511 nm).

Electronic Absorption Spectra. The visible–UV spectra of the polypyridine ruthenium(II) complexes prepared in this work (Table III) are typical for complexes of this type.[11,12] All *cis*- and *trans*-bis(thioether) complexes feature an absorption at about 425 nm, which is assigned to a Ru 4d$_\pi$ to bpy π^* metal-to-ligand charge-transfer (MLCT) band. This band occurs at essentially the same energy for the members of the bis(phenothiazine), bis(10-methylphenothiazine), and bis(dimethyl sulfide)[12] cis/trans pairs but at slightly different energies for the members of the bis(methyl phenyl sulfide) cis/trans pair (421 nm for cis versus 430 nm for trans; Table III). It is the latter behavior, wherein the band for the cis isomer occurs at higher energy than that for the trans isomer, that has been more commonly observed for previously studied cis/trans pairs.[31] This phenomenon has been ascribed to the d$_\pi$ levels of the cis isomer being more stable than those of the trans isomer because of the enhanced π stabilization engendered by having the strong bpy π acids trans to the weak ancillary π acids rather than trans to each other.[12] The fact that this effect is very small, or nonexistent, for the thioether derivatives implies that in these complexes the thioether ligands function as reasonably strong π acids.

The overall formal charge on the thioether complexes affects the energy of the MLCT band in the expected fashion.[11,12] Since it requires less energy to remove an electron from a lower charged metal center, the MLCT bands for the monocationic thioether complexes occur at lower energies (ca. 490 nm) than do those for the dicationic bis(thioether) complexes (ca. 425 nm).

Electrochemistry. The electrochemistry of polypyridine ruthenium(II) complexes containing simple thioether ligands is relatively straightforward;[11,12] the anodic region is dominated by a reversible Ru(II)/Ru(III) couple, while the cathodic region exhibits reversible waves resulting from reduction of the coordinated bipyridine ligands.[11–13,32–34] This is the situation observed with the MPS complexes *cis*- and *trans*-[(bpy)$_2$(MPS)$_2$Ru]$^{2+}$, *cis*-[(bpy)$_2$(MPS)RuCl]$^+$, and [(terpy)(MPS)$_2$RuCl]$^+$ (Table II). For the well-behaved *cis*- and *trans*-[(bpy)$_2$(MPS)$_2$Ru]$^{2+}$ complexes, the cis form is harder to oxidize by about 40 mV (Table II). This is consistent with the view that the Ru(II) form of the cis complex enjoys more effective π stabilization than does the trans complex.[12] The lower formal charge on the [(terpy)-(MPS)$_2$RuCl]$^+$ and *cis*-[(bpy)$_2$(MPS)RuCl]$^+$ complexes causes them to be oxidized considerably more easily (ca. 600 mV) than the dicationic bis(methyl phenyl sulfide) complexes.

However, when the thioether complex contains a redox-active ligand such as phenothiazine, the electrochemistry becomes much more complicated.[12] For example, reversible oxidation of [(ter-py)(bpy)(PTZ)Ru]$^{2+}$ at 1.19 V in acetonitrile leads rapidly to [(terpy)(CH$_3$CN)Ru]$^{2+}$, which can be detected by its reversible wave at 1.30 V.[4] The PTZ ligand is presumably lost as the relatively stable cation radical, PTZ$^{\bullet+}$,[35–37] and free PTZ can be detected in solution by means of its electrochemical activity at ca. 0.59 V. It should be noted that the PTZ$^{\bullet+}$ cation radical is itself redox-active[12] and can undergo a variety of dimerization, disproportionation, protonation, etc. reactions.[35–41]

(30) Heeg, M. J.; Kroener, R.; Deutsch, E. *Acta Crystallogr., Sect. C: Cryst. Struct. Commun.* **1985,** *C41,* 684.

(31) Walsh, J. L.; Durham, B. *Inorg. Chem.* **1982,** *21,* 329.
(32) Tokel-Takvoryan, N. E.; Hemmingway, R. E.; Bird, A. J. *J. Am. Chem. Soc.* **1973,** *95,* 6582.
(33) Motten, A. G.; Hanck, K.; DeArmond, M. K. *Chem. Phys. Lett.* **1981,** *79,* 541.
(34) Carlin, C. M.; DeArmond, M. K. *Chem. Phys. Lett.* **1982,** *89,* 297.
(35) Tozer, T. N.; Tuck, L. D. *J. Pharm. Sci.* **1965,** *54,* 1169.
(36) Billon, J.-P. *Ann. Chim. (Paris)* **1962,** *7,* 183.
(37) Hanson, P.; Norman, R. O. C. *J. Chem. Soc., Perkin Trans. 2* **1973,** 264 and references therein.
(38) Cheng, H. Y.; Sackett, P. H.; McCreery, R. L. *J. Am. Chem. Soc.* **1978,** *100,* 962.

The electrochemical behavior of both *cis-* and *trans-*[(bpy)$_2$(PTZ)$_2$Ru]$^{2+}$ is qualitatively similar to that of [(terpy)(bpy)(PTZ)Ru]$^{2+}$. Initial oxidation at about 1.13 V leads quickly to [(bpy)$_2$(CH$_3$CN)$_2$Ru]$^{2+}$, which undergoes reversible oxidation to Ru(III) at 1.43 V (for both the *cis-* and *trans-*bis(acetonitrile) complexes the reversible Ru(III)/Ru(II) couple is reported to be 1.44 V[31]). Since there is no noticeable change in the cyclic voltammogram at scan rates up to 400 mV/s, the rate of Ru–S bond fission in the oxidized bis(phenothiazine) complexes must be fairly rapid.

Crystal Structures. The title structures constitute the first thioether ruthenium(II) complexes to be crystallographically characterized, while the structure of the *trans-*bis(phenothiazine) complex constitutes the fourth documented example of a bis(bipyridine)ruthenium(II) complex in the trans configuration.

A survey of all structures in the Cambridge Crystallographic Database (through 1981)[45] wherein ruthenium is bonded to the sulfur atom of an organic moiety shows that the range of observed Ru–S bond lengths is 2.19–2.59 Å, with an average value of 2.38 (7) Å. This average is in good agreement with the Ru–S distances observed in this work: 2.38 (2) Å for the cis isomer and 2.347 (2) Å for the trans isomer. Similarly, a range of typically observed Ru–N(bpy) bond lengths (2.0–2.12 Å)[30,46–52] includes the average Ru–N(bpy) lengths observed in this work: 2.073 (6) Å for the cis isomer and 2.091 (9) Å for the trans isomer. In the cis complex, there is no discernible structural trans effect induced by the coordinated thioether ligand on the Ru–N bond length; this observation supports the previously stated conclusion that in these complexes the PTZ ligand is functioning as a reasonably strong π acid. Overall, the differences in Ru–ligand bond lengths between the two isomers are small but are in the direction expected from steric interactions among the bpy and PTZ ligands. Thus, the longer Ru–N bond length ($\Delta = 0.018$ (11) Å) is observed in the trans isomer, where the intraligand repulsions occur primarily between the bpy ligands, while the longer Ru–S bond length ($\Delta = 0.034$ (16) Å) is observed in the cis isomer, where the intraligand repulsions occur primarily between the bpy and PTZ ligands. Close intraligand contacts are illustrated in Figures 2 and A[53] for the cis isomer and in Figures B[53] and C[53] for the trans isomer.

In both structures the two planar aromatic rings of the phenothiazine ligand are folded to yield an overall butterfly shape; in the cis complex the dihedral angles are 150.9 (5), 150.9 (5), 156.3 (6), and 145.7 (5)°, while in the trans complex these angles are 156.9 (2) and 156.0 (2)°. The sulfur atom is significantly displaced from the aromatic planes (with displacements ranging over 0.16–0.27 Å in the cis complex and over 0.11–0.28 Å in the trans isomer), while the nitrogen atom is displaced to a lesser extent

(39) Bancroft, E. E.; Pemberton, J. E.; Blount, H. N. *J. Phys. Chem.* **1980**, *84*, 2557.

(40) Jarbawi, T. B.; Heineman, W. R. *J. Electroanal. Chem. Interfacial Electrochem.* **1982**, *132*, 323.

(41) Hamerich, O.; Parker, V. D. *Acta Chem. Scand., Sect. B* **1982**, *B36*, 59.

(42) Lai, T.-F.; Poon, C.-K. *J. Chem. Soc., Dalton Trans.* **1982**, 1465.

(43) Bucknor, S. M.; Draganiac, M.; Rauchfuss, T. B.; Ruffing, C. J.; Fultz, W. C.; Rheingold, A. L. *J. Am. Chem. Soc.* **1984**, *106*, 5379.

(44) Cordes, A. W.; Durham, B.; Swepston, P. N.; Pennington, W. T.; Condren, S. M.; Jensen, R.; Walsh, J. L. *J. Coord. Chem.* **1982**, *11*, 251.

(45) "Cambridge Structural Database"; Cambridge Crystallographic Data Centre, University Chemical Laboratory: Cambridge, England, 1987.

(46) Rillema, D. P.; Jones, D. S.; Levy, H. A. *J. Chem. Soc., Chem. Commun.* **1979**, 849.

(47) Phelps, D. W.; Kahn, E. M.; Hodgson, D. J. *Inorg. Chem.* **1975**, *14*, 2486.

(48) Clear, J. M.; Kelly, J. M.; O'Connell, C. M.; Vos, J. G.; Cardin, C. J.; Costa, S. R. *J. Chem. Soc., Chem. Commun.* **1980**, 750.

(49) Durham, B.; Wilson, S. R.; Hodgson, D. J.; Meyer, T. J. *J. Am. Chem. Soc.* **1980**, *102*, 600.

(50) Stephens, F. S.; Vagg, R. S.; Williams, P. A. *Inorg. Chim. Acta* **1983**, *72*, 253.

(51) Kimura, T.; Sakurai, T.; Shima, M.; Nagai, T.; Mizumachi, K.; Ishimori, T. *Acta Crystallogr., Sect. B: Struct. Crystallogr. Cryst. Chem.* **1982**, *B38*, 112.

(52) Templeton, J. L. *J. Am. Chem. Soc.* **1979**, *101*, 4906.

(53) All figures and tables with letter designations have been deposited as supplementary material.

Table X. Angular Analyses[a] for *cis-* and *trans-*[(bpy)$_2$(PTZ)$_2$Ru]$^{2+}$

Bpy Intraligand Angles

	twist angle about bridging C atoms, τ[b]	py–py dihedral angle 2θ
	cis	
bpy 1 (C5, C6)	2.1	9.2
bpy 2 (C15, C16)	0.4	5.1
bpy 3 (C49, C50)	−2.7	5.9
bpy 4 (C59, C60)	0.8	2.1
	trans	
bpy 1 (C5, C6)	−2.0	16.8
bpy 2 (C27, C28)	4.8	12.2

Interligand Twist Angle about Ru–S Bond, ϕ[c]

	Cis	
(S1, Ru1)		0.4
(S2, Ru1)		2.2
(S3, Ru2)		2.9
(S4, Ru2)		3.1
	Trans	
(S1, Ru1)		22.1
(S2, Ru2)		12.9

[a] Angles given in degrees. [b] $\tau = \frac{1}{2}[\omega(N-C-C-N) + \omega(C-C-C-C)]$. [c] $\phi = \frac{1}{2}[\omega(C-S-Ru-N) + \omega(C'-S-Ru-N')]$.

(0.02–0.13 Å in the cis complex and 0.01–0.03 Å in the trans isomer). This butterfly conformation is also observed for the free ligand,[51] which exhibits a dihedral angle of 158.5° and displacements of 0.183 and 0.035 Å for the sulfur and nitrogen atoms, respectively.

Bond lengths and bond angles within the two coordinated PTZ ligands are equal within error for both the cis and trans isomers. Figure D[53] presents averaged values for both isomers. These averaged values are in good agreement with the comparable values observed for the free PTZ ligand:[51] the largest difference in bond length is observed for the S–C bond (1.762 (6) Å for the free ligand vs 1.772 (9) and 1.78 (1) Å for the average trans and cis ligands); the largest difference in bond angle is observed for the C–N–C angle (124.4 (5)° for the free ligand vs 122.2 (7) and 122.3 (8)° for the average trans and cis ligands).

The bond angles and distances within the bpy ligands are in good agreement with accepted literature values.[30,43–49] Table X presents two parameters that gauge the distortions of bipyridine groups: 2θ is the dihedral angle between the two planes of the pyridine halves of the molecule, and τ (twist angle) is the average of the two torsion angles across the C–C bond bridging the pyridine halves. *trans-*Bis(bipyridine) complexes are necessarily distorted in either a bowed or twist conformation, the net result of which is to separate the α-hydrogen atoms of opposing ligands. Whenever the central metal ion occupies an inversion center, the twist distortion does not provide steric relief and the bowed conformation is the only one reasonably allowed.[49] As illustrated in Table X, *trans-*[(bpy)$_2$(PTZ)$_2$Ru]$^{2+}$ exhibits a marked bowing of the bpy ligands, characterized by large 2θ angles and small twist angles. The cis isomer also possesses bowed bpy ligands, although to a much lesser extent. In each case, the direction of the bow of the bpy ligand follows the contour of the PTZ fold on which it is stacked.

The angles between the S–N vector of a PTZ ligand and the adjoining mean bpy plane are 16.7 (3), 17.6 (3), 15.3 (3), and 15.8 (3)° in *cis-*[(bpy)$_2$(PTZ)$_2$Ru]$^{2+}$, while the independent values in the trans isomer are 32.3 (4) and 29.7 (4)°. These values illustrate that the tetrahedral coordination requirements of the sulfur atom force the PTZ ligand to tilt with respect to the bpy plane; this causes the atoms on the sulfur side of the PTZ ligand to lie closer to the associated bpy ligand than do the atoms on the nitrogen side of the PTZ ligand. Free rotation about the Ru–S bond implies that the stacking between the ligands is due either to efficiency or to a π–π interaction. A twist angle ϕ (analogous to τ) can be defined to describe the degree to which the ligand centers overlap: $\phi = \frac{1}{2}[\omega(C-S-Ru-N) + \omega(C'-S-Ru-N')]$.

Table X lists these ϕ values and shows that the overlap between the ligands is fairly closely matched in the cis isomer. Contrariwise, ϕ values are substantially larger in the trans complex, where steric restrictions on PTZ are less stringent. Figures 2 and A[53] illustrate the overlap for the cis isomer, while Figures B[53] and C[53] illustrate the overlap for the trans isomer. Distances between the atoms of PTZ and the associated mean bpy plane average 3.2 (5) Å in the cis isomer and 3.0 (7) Å in the trans isomer. Since these interligand stacking distances are of the same magnitude as those observed (3.37 Å)[54,55] when PTZ associates with aromatic molecules in the solid state, it is possible that they reflect strong π–π attraction between the PTZ and bpy ligands. Such interligand stacking phenomena may be of interest to the design and synthesis of molecular conductors.

In both structures, each independent (PTZ)N–H group is involved in a strong hydrogen bond to either a fluorine atom of

hexafluorophosphate or to the solvated water molecule. In the cis complex these values are HN12···O(w) = 2.115 Å, HN5···F9 = 2.327 Å, HN6···F12 = 2.127 Å, and HN11···F6 = 2.366 Å; in the trans complex they are HN6···O1 = 1.882 Å and HN3···F12 = 2.291 Å.

Supplementary Material Available: Thermal parameters (Table A for cis and Table B for trans), hydrogen positional parameters (Table C for cis and Table D for trans), bond lengths (Table E for cis and Table F for trans), bond angles (Table G for cis and Table H for trans), least-squares planes (Table I for cis and Table J for trans), PLUTO drawings of the cis (Figure A) and trans complexes (Figures B and C), and average bond lengths and angles in the coordinated PTZ ligands (Figure D) (29 pages); observed and calculated structure factors (Table K for cis and Table L for trans) (84 pages). Ordering information is given on any current masthead page.

(54) McDowell, J. J. H. *Acta Crystallogr., Sect. B: Struct. Crystallogr. Cryst. Chem.* **1976,** *B32,* 5.
(55) Herbstein, F. H. *Perspect. Struct. Chem.* **1971,** *4,* 166.

Contribution from the Institute for Molecular Science, Okazaki National Research Institutes, Myodaiji, Okazaki 444, Japan, and Department of Chemistry, Nagoya University, Chikusa, Nagoya 464, Japan

BINAP–Ruthenium(II) Dicarboxylate Complexes: New, Highly Efficient Catalysts for Asymmetric Hydrogenations

Tetsuo Ohta,[1a] Hidemasa Takaya,*[1a] and Ryoji Noyori*[1b]

The BINAP–ruthenium(II) complexes Ru(OCOR)₂[(R)- or (S)-2,2′-bis(diarylphosphino)-1,1′-binaphthyl] [aryl = phenyl, p-tolyl; R = CH₃, C(CH₃)₃] have been prepared. The crystal structure of Ru[OCOC(CH₃)₃]₂[(S)-2,2′-bis(diphenylphosphino)-1,1′-binaphthyl], determined by X-ray crystallography [diffraction data collected at –60 °C, formula C₅₄H₅₀O₄P₂Ru, monoclinic, space group $P2_1$, $Z = 2$, $a = 13.272$ (2) Å, $b = 16.224$ (3) Å, $c = 12.701$ (2) Å, $\beta = 124.34$ (1)°, $R = 0.037$, $R_w = 0.043$], indicates that the monomeric ruthenium(II) complex has a distorted octahedron coordination geometry involving two phosphorus atoms of BINAP and four oxygen atoms of pivalate ligands. The complex has a Λ structure, while the BINAP-containing seven-membered chelate ring is fixed in a δ conformation. The molecular structure has been compared with that of Rh[(R)-BINAP](norbornadiene)ClO₄. These BINAP–ruthenium complexes serve as highly efficient catalysts for asymmetric hydrogenations of various enamides, α-(acylamino)acrylic acids, α,β- and β,γ-unsaturated carboxylic acids, allylic and homoallylic alcohols, α-amino ketones, etc.

Introduction

Homogeneous asymmetric hydrogenation with transition metal complexes possessing chiral ditertiary phosphine ligands provides a powerful tool for chemical multiplication of chirality. So far the highly stereoselective reactions have been achieved mainly by the Rh(I)-based complexes. We here report synthesis and structures of new mononuclear Ru(II) complexes (**3**) containing axially dissymmetric (R)- or (S)-2,2′-bis(diphenylphosphino)-1,1′-binaphthyl [(R)- or (S)-BINAP] and its derivatives (**1** and **2**).[2] These complexes exhibit very high catalytic activity and enantioselectivity in hydrogenation of a wide range of substrates such as enamides,[3] α-(acylamino)acrylic acids,[4] alkyl- and aryl-substituted acrylic acids,[5] β,γ-unsaturated carboxylic acids,[5]
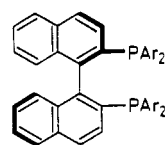
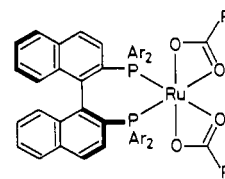
(R)-1: Ar = C₆H₅
(R)-2: Ar = p-CH₃C₆H₄
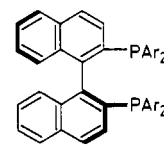
(S)-1: Ar = C₆H₅
(S)-2: Ar = p-CH₃C₆H₄
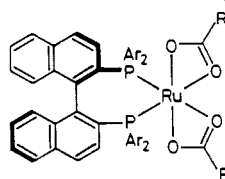
Δ-(R)-3   Λ-(S)-3

a: R = CH₃, Ar = C₆H₅
b: R = (CH₃)₃C, Ar = C₆H₅
c: R = CH₃, Ar = p-CH₃C₆H₄

(1) (a) Okazaki National Research Institutes. (b) Nagoya University.
(2) (a) Miyashita, A.; Yasuda, A.; Takaya, H.; Toriumi, K.; Ito, T.; Souchi, T.; Noyori, R. *J. Am. Chem. Soc.* **1980,** *102,* 7932. (b) Miyashita, A.; Takaya, H.; Souchi, T.; Noyori, R. *Tetrahedron* **1984,** *40,* 1245. (c) Takaya, H.; Mashima, K.; Koyano, K.; Yagi, M.; Kumobayashi, H.; Taketomi, T.; Akutagawa, S.; Noyori, R. *J. Org. Chem.* **1986,** *51,* 629.
(3) Noyori, R.; Ohta, M.; Hsiao, Y.; Kitamura, M.; Ohta, T.; Takaya, H. *J. Am. Chem. Soc.* **1986,** *108,* 7117. Kitamura, M.; Hsiao, Y.; Noyori, R.; Takaya, H. *Tetrahedron Lett.* **1987,** *28,* 4829.
(4) Unpublished results. [Ru₂Cl₄(BINAP)₂]N(C₂H₅)₃ is also effective: Ikariya, T.; Ishii, Y.; Kawano, H.; Arai, T.; Saburi, M.; Yoshikawa, S.; Akutagawa, S. *J. Chem. Soc., Chem. Commun.* **1985,** 922.
(5) Ohta, T.; Takaya, H.; Kitamura, M.; Nagai, K.; Noyori, R. *J. Org. Chem.* **1987,** *52,* 3174.

allylic and homoallylic alcohols,[6] α-amino ketones,[7] etc.[8] The Ru complexes are in many cases superior to the corresponding